Macromolecules

Article

pubs.acs.org/Macromolecules

Porous Films via PE/PEO Cocontinuous Blends

Milana Trifkovic,[†] Aaron Hedegaard,[†] Kyle Huston,[†] Mehdi Sheikhzadeh,[‡] and Christopher W. Macosko*,[†]

[†]Department of Chemical Engineering and Materials Science, University of Minnesota, Minneapolis, Minnesota 55455, United States

[‡]Instrumentation & Control Engineering Technology, Lambton College, Sarnia, Canada N7S 6K4

Supporting Information

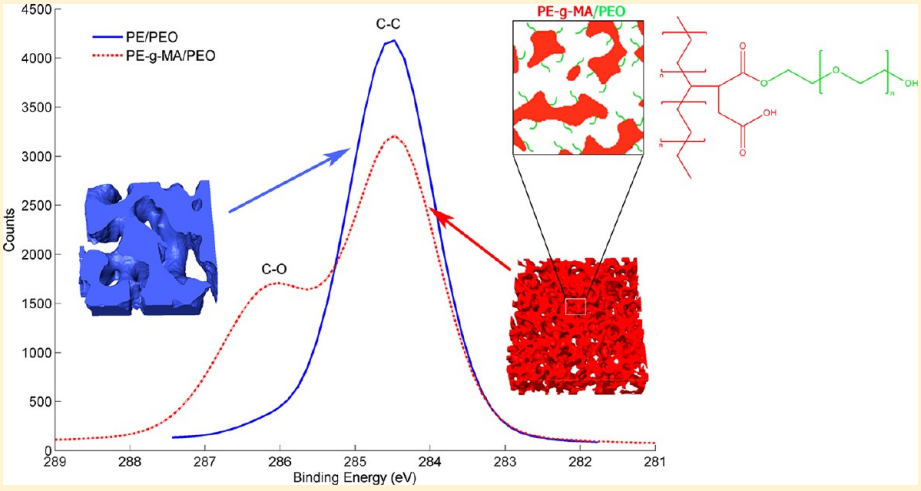

ABSTRACT: The design of a porous membrane support layer derived from cocontinuous polymer blends is presented. We investigate the effect of blend composition, shear rate, residence time, and annealing time on the cocontinuous morphology of polyethylene (PE)/poly(ethylene oxide) (PEO) blends. Porous PE sheets were generated by water extraction of PEO and used as a support layer for gas separation membranes. The PE/PEO blends using nonfunctional and maleic anhydride functional PE (PE-*g*-MA) were mixed in a batch microcompounder and in a pilot plant scale corotating twin-screw extruder. Using PE-*g*-MA resulted in pore size reduction from 10 to 2 μm and suppression of coarsening of the morphology during further annealing of the blends due to formation of PE−PEO graft copolymers. Equilibrium interfacial tension, estimated by fitting the rheology of droplet blends to the Palierne viscoelastic droplet model, was 3 and 0.4 mN/m for PE/PEO and PE-*g*-MA/PEO systems, respectively. The specific interfacial area and phase size distribution were calculated from 3D images acquired by laser scanning electron microscopy (LSCM). We prepared gas separation membranes by solvent casting an acetone solution of ionic gel into porous PE sheets and discussed the effect of type of processing, average pore size, pore size distribution, and pore wall functionality on their performance.

INTRODUCTION

Melt blending of polymers is an effective way to obtain materials with enhanced properties, specifically processability, mechanical and electrical properties, and barrier behavior. A significant effort has been made to control the morphology of blends, which has been found to have a great impact on their properties. Most polymers used in blends are immiscible or partially miscible due to their high molecular weight and unfavorable interactions, and thus their blends macrophase separate into heterogeneous morphologies, including droplet/matrix, fiber, lamella, and cocontinuous.[1] The type of morphology formed during processing depends on the physical properties of the polymers (interfacial tension, viscosities, and the ratio of these viscosities), their volume fractions, and the processing conditions.[2] Of all possible morphologies, the cocontinuous morphology shows a unique combination of the characteristics of both polymer components.[3]

A cocontinuous morphology is a nonequilibrium morphology defined by the coexistence of at least two continuous structures within the same volume. As such, it is an unstable morphology, and it starts changing through self-similar coarsening, filament breakup, and retraction, as soon as the fluid blend comes out of the melt compounder. In order to maintain the desired cocontinuous morphology, the blend is quenched immediately after processing to freeze the morphology.

Received: February 14, 2012
Revised: June 30, 2012
Published: July 19, 2012

Table 1. Material Properties

material	M_w (g/mol)	M_w/M_n	functionality groups/chain	η_0, (Pa s), at 150 °C	η, (Pa s), at 400 s^{-1}	density (g/cm^3), at 23 °C
PE	5.9×10^4	5.0	0	2.26×10^4	340	0.923
PE-*g*-MA	7.9×10^4	5.86	12.9	8.00×10^4	540	0.96
PEO	1×10^5	4.5	2	1.05×10^4	410	1.2

Interfacial modifiers called compatibilizers are often added to blends in order to stabilize their morphology by suppressing coarsening[8−10] and enhancing interfacial adhesion. This also typically results in a significant size reduction in the phase domains of the blend. Typical compatibilizing molecules are block or graft copolymers, which contain a block miscible with each phase, often formed *in situ* during the mixing process via coupling reactions between functional groups at the interface of the two phases.[4−7] This *in situ* approach, called reactive compatibilization, is usually preferred in industry.[3]

Because of the irregular shape of the microstructure, quantitative morphological characterization of cocontinuous blends is a challenge. The interfacial area per unit volume is often used in modeling the evolution of interface shape and the characteristic phase size of the blend.[11,12] In most studies, interfacial perimeter per area of two-dimensional cross sections of blends, imaged by scanning electron microscopy (SEM) or transmission electron microscopy (TEM), is used to describe the interfacial shape. However, this often fails to describe the true morphology due to the nonuniformity of the blend. Recently, improvements have been made in three-dimensional imaging of polymer blends using various technologies including transmission electron microtomography (TEMT),[13,14] X-ray phase tomography,[15,16] three-dimensional nuclear magnetic resonance (NMR) imaging,[17] and laser scanning confocal microscopy (LSCM).[12,18] LSCM in particular has the advantages of fast and nondestructive image acquisition. However, in order to acquire a stack of 2D images, at least one of the phases must fluoresce, and the sample must be optically transparent to provide an adequate depth of field. To satisfy the fluorescence requirement, one of the polymers is usually polymerized with a small quantity of a fluorescent monomer.[12] However, this is not a feasible option for studies that employ most commercially available polymers. To satisfy the optically transparent requirement, the phases must match in terms of refractive index.

The present study explores the application of porous polyethylene films derived from polyethylene/poly(ethylene oxide) (PE/PEO) cocontinuous blends as a support for gas separation membranes. The polymer system was chosen on a basis of ease of extraction of one of the phases (PEO in this case due to its high solubility in water) and the tough mechanical properties, solvent resistance, and low cost of PE.

This work reports the effect of functionalization of polyethylene, blend composition, and processing conditions on the blend morphology. Rheological characterization of droplet blends was fit to the Palierne viscoelastic droplet model[19] to quantify the equilibrium interfacial tension of PE/PEO blends. LSCM was used for 3D imaging and qualitative and quantitative analysis of cocontinuous blend morphology.

Gas separation membranes were prepared by solvent casting an acetone solution of poly(vinylidene fluoride-*co*-hexafluoropropylene) (p(VDF−HFP)) swollen with 1-ethyl-3-methylimidazolium bis(trifluoromethylsulfonyl)imide ([EMIM][TFSI]) into porous polyethylene films and tested in a gas diffusion cell.[20,21] To demonstrate the possibility of generating a cocontinuous structure on a large scale, the process was scaled up from the 4 g batch microcompounder to a pilot-plant scale twin-screw extruder.

EXPERIMENTAL SECTION

Materials. Table 1 shows blend component properties. Low-density polyethylene (PE) was provided by the Dow Chemical Company (LDPE 9955i), maleic anhydride grafted polyethylene (PE-*g*-MA) containing 1.6 wt % maleic anhydride by Chemtura (Polybond 3029), and poly(ethylene oxide) (PEO) by the Dow Chemical Company (Polyox N10). Complex viscosity profiles of PE-*g*-MA, PE, and PEO along with their Cross model fits are shown in Figure 1.

$$\frac{\eta - \eta_\infty}{\eta_0 - \eta_\infty} = \frac{1}{1 + (K\dot{\gamma})^{1-n}} \quad (1)$$

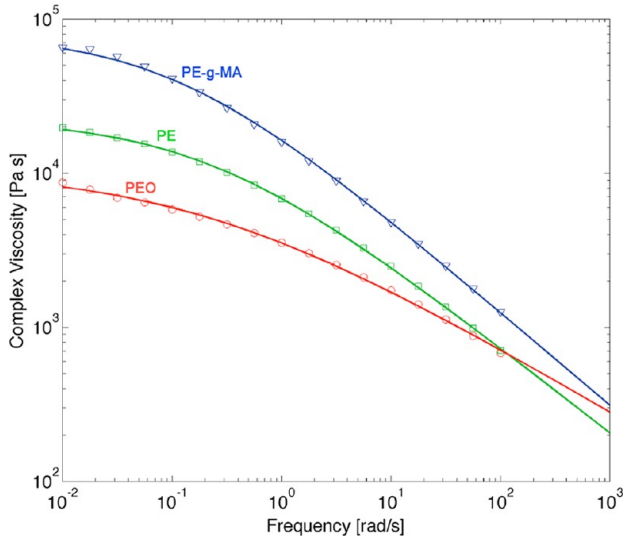

Figure 1. Complex viscosity of pure materials (lines represent Cross model fits, eq 1).

The corresponding Cross model parameters are shown in Table 2. For all samples, η_∞ was assumed to be zero. In order to apply the Cross model fitting, the Cox−Merz relationship was assumed to hold, such that the measured frequency-dependent complex viscosity of the materials was equivalent to the shear rate-dependent viscosity for $\omega = \dot{\gamma}$.[22] Molecular weights of the polyethylenes used in this study were measured by high-temperature gel permeation chromatography at 155 °C using 1,2,4-trichlorobenzene as eluent (Table 1) and polystyrene standards. Density values in Table 1 were provided by the manufacturer. 2-Hydroxyethyl methacrylate (HEMA) monomer was purchased from Aldrich and was mixed with 1 wt % azobis-

Table 2. Cross Model Parameters

material	η_0, (Pa s)	n	K (s)
PE	2.26×10^4	0.442	4.45
PE-*g*-MA	8.00×10^4	0.395	9.44
PEO	1.05×10^4	0.578	4.95

dx.doi.org/10.1021/ma300293v | *Macromolecules* 2012, 45, 6036−6044

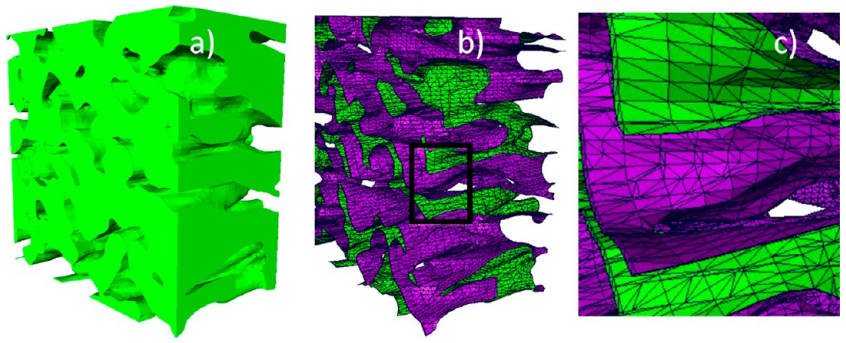

Figure 2. Rendered 3D microstructure for PE/PEO blend: (a) solid model of the PE microstructure, (b) interface between blend phases (purple facing toward the PEO phase and green toward PE phase), (c) detail of the meshed interface (from the black square in (b)).

(isobutyronitrile), a thermally activated radical initiator, also purchased from Aldrich. Both were used as received.

Blend Preparation and Annealing. Blends were prepared by both batch and continuous melt mixing processes. Batch melt compounding of PE/PEO and PE-*g*-MA/PEO was performed in a recirculating, conical twin-screw extruder (Microcompounder, DACA Instruments) at a rotor speed of 200 rpm and 150 °C. The weight ratio of PE/PEO and PE-*g*-MA/PEO was varied between 55/45 and 45/55. Upon completion of batch mixing, the blends were rapidly quenched in liquid nitrogen to freeze the morphology.

Continuous melt mixing was performed in a pilot plant scale corotating twin-screw extruder (Leistritz, Neuremberg, Germany) with screw diameter of 27 mm, L/D of 48:1, and 12 individually heated/cooled zones. The extruder was operated with the total feed rate of 5 kg/h, a barrel/die set temperature of 150 °C, and screw rotational speed of 200 rpm, while varying the weight ratio of PE/PEO (in the same fashion as for the batch process) and the PEO introduction zone (zone 1 and zone 5). Two different screw configurations were used to subject the molten blends to high-intensity and medium-intensity mixing conditions (see Supporting Information). Residence time was varied from about 80 to 50 s for lower shear configuration and 120 to 70 s for high shear configuration by introducing PEO in zone 5. Two gravimetric feeders (Brabender, Missisagua, Canada) with the feed rate range of 1−10 and 0.5−3 kg/h were used for feeding materials. The extruded strands were quenched in liquid nitrogen. During experimental studies, sensors located on the extruder continuously measured processing conditions. A detailed description of the extrusion experimental setup can be found elsewhere.[23]

Small pieces (0.7−1 g) of the resulting blends were placed between sheets of fluoropolymer coated fabric (Premium 6 Mil, American Durafilm) and then placed between the heated metal platens of a compression press (Carver, Inc., Wabash, IN). For morphology coarsening analysis, samples were annealed for various time intervals at 150 °C with no applied pressure. To obtain 100 μm thin films, samples were pressed for no more than 3 min. After annealing, cold water was flushed through the press platens to cool the samples to room temperature.

Rheological Characterization. Rheological measurements of the blends and blend components were carried out at 150 °C using an ARES (TA Instruments) rheometer with a 25 mm parallel plate geometry. Prior to further rheological characterization, dynamic strain sweep tests were performed on all materials to determine the critical strain at which each material began to exhibit nonlinear viscoelasticity. All subsequent tests were performed at strains within the linear viscoelastic region of the material. Small-amplitude oscillatory shear tests were performed over a frequency range of 100−0.01 rad/s.

Morphology Analysis. Samples were cryo-microtomed (Reichert UltraCut S ultramicrotome) at −140 °C using a glass knife. Phase contrast was generated by immersing the samples in water for 24 h and extracting the PEO phase, yielding porous PE samples. Samples were then sputter-coated with 50 Å of platinum. A scanning electron microscope (SEM, JEOL 6500) was used at an accelerating voltage of 5 kV and a working distance of 10 mm to study the morphology and phase dimensions after extraction.

Laser scanning confocal microscopy (LSCM, Olympus Fluo View 1000) was employed to obtain 3D images of cocontinuous polymer blends. In order to satisfy the LSCM requirements of specimen transparency and fluorescence of one phase, hydroxyethyl methacrylate (HEMA) with 0.01 wt % rhodamine B dye was polymerized inside of the pores of the porous PE film at 80 °C for 10 min. An incident laser beam of wavelength of 563 nm excited fluorescence from the rhodamine dye dissolved in polyHEMA. A detector above the stage was set only to allow the rhodamine flourescense through the filter. Hence, the polyHEMA phase, which represents the previously extracted PEO phase, was identified as the bright phase under the LSCM. An oil-immersed 60× objective lens was used with LSCM to obtain a stack of optical micrographs. The focal depth increment, Δz, was varied between 0.3 and 0.7 μm, depending on the average pore size of the sample.

The numerical models for the structural analysis were created in Matlab 7 (The MathWorks Inc.) using visualization toolbox. The LSCM images were imported, material pixels are separated from void pixels based on their gray values (tresholding), and a binary image representing the structure was obtained. A common practice for segmentation is to choose a simple global threshold. However, this procedure may lead to biases when one is trying to segment a stack of LSCM images. The distinction between the void and solid phases in images frequently changes throughout the stack of images since the laser's intensity is weakened as it penetrates deeper into the sample. For this reason, the iterative selection thresholding method was used to perform segmentation of the cocontinuous blend images into pores and solid polymer material.[24]

The 3D image was reconstructed using Avizo (v. 6.3) interactive visualization package. A marching cubes algorithm was applied for triangular mesh generation. Interfacial area per unit volume, Q, was obtained by adding the areas of all the triangles A_i of the generated mesh and dividing the sum by the total volume of the sample, V.[25]

$$Q = \frac{1}{V}\sum_{i=1}^{N} A_i \tag{2}$$

Figure 2 shows (a) "solid model" of PE phase, and (b) the interface between PEO and PE phase rendered and meshed by applying marching cubes algorithm.

In addition to interfacial area, pore size distribution is another important descriptor of porous films derived from cocontinuous blends. Since the pores can be identified from contiguous white or black regions in a binarized image using MATLAB visualization toolbox, the pore size distribution can be estimated. Having identified the pores and their areas in each plane through the entire thickness, the perimeter of each pore is then calculated by identifying the set of pixels that belong to the pore and have at least one neighbor that interfaces with a polyethylene pixel. Pore size distribution is calculated based on the equivalent pore diameter, which is the diameter of a circle with the same area as the pore under consideration:[26]

$$D_{eq,i} = \frac{4A_{p,i}}{P_i} \quad (3)$$

where A_p is the pore area and P is its perimeter. The volume of each pore identified is calculated by multiplying the area of that pore by the constant slice thickness. By stacking up the volume occupied by pores of a given equivalent diameter for all slices through the thickness, the overall pore size distribution for a sample can be obtained. At least 200 pores were sized for each distribution.

X-ray Photoelectron Spectroscopy. XPS was used for elemental analysis to detect grafted polymer at the surface of the blends. XPS spectra were collected using a SSX-100 spectrometer from Surface Science Instruments using monochromatic Al Kα X-rays with an accelerating voltage of 10 kV and a current of 20 mA. The X-ray beam spot size was 200 μm. A metal mesh and low-energy electron gun (energy output was tuned between 10 and 20 eV, dependent on the sample and spectra range) were used to provide charge neutralization during the experiment.

Contact Angle Measurement. Static contact angle measurements were conducted using the captive air bubble method. The advantage of the captive bubble over the sessile drop method is complete hydration of the sample, and thus, the surface energy of interest between water and the film should not change with the time of measurement. Measurements were done on porous PE films obtained from the pressed blends, followed by PEO extraction. Porous films were placed in deionized water and air bubbles were released beneath the PE film using a J-shaped needle. The porosity of both samples was 50% in this case. The bubble trapped under the surface of the film was imaged with a contact angle meter DM-CE1 (Kyowa, Japan) and the tangent contact angle determined using built in FAMAS (v 3.1.3) analyzing software. The lower the air bubble contact angle the more hydrophilic the surface. The average static contact angles and 95% confidence intervals were obtained using at least 10 gas bubbles on each specimen and are reported in Table 3. A solid (nonporous) PE and PE-*g*-MA films have much larger contact angles in comparison to their corresponding porous films. This happens since pores draw water in by capillary forces, resulting in Wenzel wetting.[27]

Table 3. Water Contact Angles for PE Films

	smooth films		porous films	
material	PE	PE-*g*-MA	PE	PE-*g*-MA
water contact angle (deg)	81 ± 3	63 ± 2	27 ± 2	18 ± 2

Palierne Model. The rheological behavior of immiscible polymer blends is generally complex, where the rheological properties depend strongly on composition and viscoelastic properties of the components. Under oscillatory shear flow or cessation of shear, the blend modulus, G^*, can be determined by contribution of each component and the interfacial tension:

$$G^* = G^*_{components} + G^*_{interface} \quad (4)$$

Palierne[19] suggested a model for droplet blends such that the modulus of a blend can be determined from that of each component. The model takes into account the size of the viscoelastic droplets dispersed in a viscoelastic matrix, the interfacial tension between the components, Γ, and interfacial shear modulus, β_s, and dilatation modulus, β_d.

$$G^* = G^*_m\left(\frac{1+\frac{3\phi E}{2D}}{1-\frac{\phi E}{D}}\right) \quad (5)$$

$$E = 2(G^*_d - G^*_m)(19G^*_d + 16G^*_m) + \frac{48\beta^*_d\Gamma}{R_{avg}^2} + \frac{32\beta^*_s(\Gamma+\beta^*_d)}{R_{avg}^2} + \frac{8\Gamma}{R_{avg}}(5G^*_d + 2G^*_m) + \frac{2\beta^*_d}{R_{avg}}(23G^*_d - 16G^*_m) + \frac{4\beta^*_d}{R_{avg}}(13G^*_d + 8G^*_m) \quad (6)$$

$$D = (2G^*_d + 3G^*_m)(19G^*_d + 16G^*_m) + \frac{48\beta^*_d\Gamma}{R_{avg}^2} + \frac{32\beta^*_s(\Gamma+\beta^*_d)}{R_{avg}^2} + \frac{40\Gamma}{R_{avg}}(G^*_d + G^*_m) + \frac{2\beta^*_d}{R_{avg}}(23G^*_d + 32G^*_m) + \frac{4\beta^*_s}{R_{avg}}(13G^*_d + 12G^*_m) \quad (7)$$

E and D are functions, which contain all model parameters. G^*, G^*_d, G^*_m are the complex moduli of the blend, dispersed phase, and matrix, respectively. φ is the volume fraction of droplets, and R_{avg} is the volume average radius of the droplet. The Palierne model allows us to predict the interfacial tension of dilute immiscible blends from the rheological measurements. Compared to the original Palierne model,[19] eqs 5−7 contain the volume average radius of the droplets instead of droplet radius size distribution.

A simplified version of the Palierne model (eqs 5−7), which assumes that $\beta_s = 0$ and $\beta_d = 0$, has successfully been applied to obtain morphological information on uncompatibilized blends by several researchers.[28−31] This simplified version was used to fit Palierne model to dynamic moduli with previously calculated R_{avg}, to estimate a single parameter interfacial tension, Γ, of uncompatibilized PE/PEO blends.

For compatibilized PE-*g*-MA/PEO blends, the more general version of the Palierne model, which accounts for interfacial shear modulus, must be used.[32] The surface shear modulus is related to the presence of the compatibilizer at the interface. Therefore, the two-parameter (Γ and β_s) version of the Palierne model which assumes $\beta_d = 0$, as discussed in detail by Van Hemelrijck et al.,[33] is used in the present work.

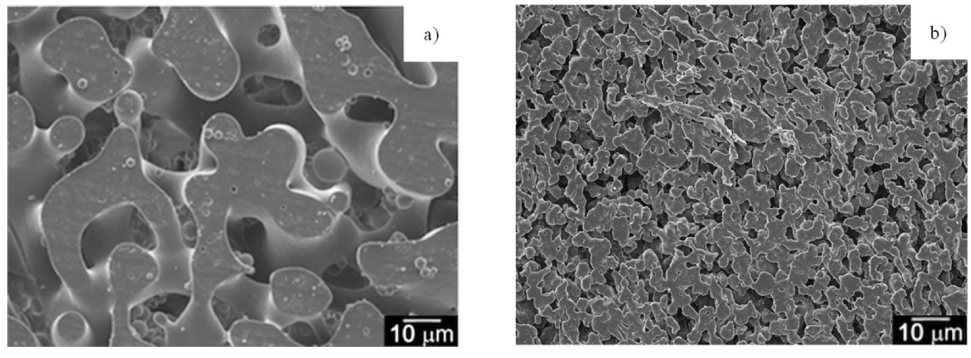

Figure 3. SEM micrographs of 50/50 vol % blends: (a) PE/PEO blend; (b) PE-*g*-MA/PEO blend.

dx.doi.org/10.1021/ma300293v | Macromolecules 2012, 45, 6036−6044

In this work, the Palierne model is used to obtain the interfacial tension between PE and PEO as well as PE-*g*-MA and PEO. Knowing the dynamic moduli G' of both components and those of the blends, the droplet size distribution of the dispersed phase at 150 °C, it is possible to determine the interfacial tension using eqs 5−7. The droplet blend composition for PE/PEO and PE-*g*-MA/PEO was 90/10 wt %. To determine the droplet size, the droplet area was traced from SEM images using Matlab software, and diameter was calculated from the corresponding droplet area, A_d. Typically, 200−300 particles were analyzed per sample. The volume average radius (R_{avg}) was calculated based on the particle size distribution.

RESULTS AND DISCUSSION

Blends with PE vs PE-*g*-MA. Figure 3 shows a comparison of PE/PEO and PE-*g*-MA/PEO of cryo-microtomed extruder strands processed in the batch microcompounder under the same conditions (T = 150 °C, RPM = 200). Significant reduction in pore size is evident. As PEO used in this study is hydroxyl-terminated on both ends, the possibility of reactive compatibilization as a consequence of reaction between maleic anhydride (MAH) groups randomly distributed along the PE backbone and OH groups at the ends of PEO chains was investigated. Tselios et al.[34] report reaction between MAH and OH groups in blends of poly(ethylene-*co*-vinyl alcohol) and styrene−maleic anhydride (SMA) based on Fourier-transform infrared spectroscopy, differential scanning calorimetry, and extraction experiments. Flores et al.[35] also observed similar functional group reaction from their investigation on blends of ethylene−vinyl acetate−vinyl alcohol and SMA.

X-ray photoelectron spectroscopy (XPS) and the corresponding 3D images of porous PE and PE-*g*-MA films obtained after PEO extraction are shown in Figure 4. The XPS high-resolution spectra depicted the presence of carbon and oxygen for both films, with C/O ratio of 55/1 and 4/1 for porous PE and porous PE-*g*-MA films, respectively. The significant oxygen content (20%) on the surface of the porous polyethylene films derived from blends with PE-*g*-MA confirmed the formation of PE-*g*-PEO graft copolymer. This in turn explains the reduced contact angle (Table 3) and the significant phase domain size reduction observed in blends using functionalized PE. The slight amount of oxygen present at the surface of porous PE film may be attributed to incomplete rinsing of PEO.

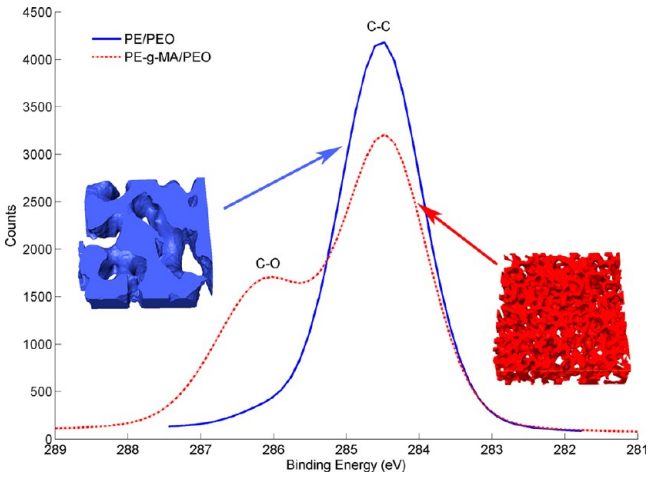

Figure 4. XPS spectra from cocontinuous blends after PEO extraction of 50/50 vol % PE-*g*-MA/PEO (right, C:O = 4:1, 1.9 μm pore size) and PE/PEO (left, C:O = 55:1, 11.1 μm pore size). The inset 3D images from laser scanning confocal microscopy (LSCM) show a 50 × 50 × 15 μm section of each porous film.

Figures 5a,b plot the characteristic length, $1/Q$, as a function of annealing time for these blends, showing the effect of graft copolymer on suppression of coarsening during annealing. The stabilization of the interface is obvious in the case of the reactively compatibilized blend as the characteristic length increased from 1.5 to 2.5 μm in the first 5 min of annealing and then stopped.

In contrast, the uncompatibilized blend shows an almost linear increase in the charactestic length. Similar difference between annealing of compatibilized and nonfunctionalized cocontinuous blends was observed previously.[9,10]

The rheology and morphology of droplet blends were investigated to determine interfacial tension. Figure 6a shows the frequency dependence of the storage moduli of pure polymers (PEO and PE) and the uncompatiblized PE/PEO droplet blend. The blend data were fit with the Palierne model using R_{avg} = 1.02 μm (obtained from the SEM image analysis) and a single parameter, Γ (interfacial tension). The estimated interfacial tension is 3 mN/m. In the case of the compatibilized PE-*g*-MA/PEO blend, the results of fitting the data using R_{avg} = 0.15 μm with the Palierne model using two parameters (Γ and β_s) is shown in Figure 6b. The dynamic responses of pure PE-*g*-MA, PEO, and the compatibilized blend subjected to the same shear history are added to this figure as well. The interfacial tension estimate is 0.4 mN/m, and the corresponding interfacial shear modulus, β_s, is 0.05 mN/m. In the case of the compatibilized blend, the inclusion of the interfacial shear modulus is necessary to account for the existence of the generated PE-*g*-PEO graft copolymers at the interface, which, as a third component of the blend, will contribute an additional elastic response to the system. On the other hand, the absence of graft copolymers in uncompatibilized blend will result in a zero interfacial modulus.

From the values of contact angle in Table 3 for the pure PE and PE-*g*-MA films, it is evident that the presence of polar maleic anhydride groups increases film's wettability, which is shown by a significant decrease of a contact angle value. Similarly, the porous films derived from cocontinuous blends with PE-*g*-MA result in improved wettability and consequently easier incorporation of an ionic gel into the film pores during the solvent casting process.

From the above comparison of PE/PEO and PE-*g*-MA/PEO blends, it can be concluded that graft copolymers formed at PE-*g*-MA/PEO interfaces. This reactive coupling resulted in a significant decrease of interfacial tension and consequently smaller phase domains in cocontinuous blends and stabilization of interface during annealing at 150 °C. For our proposed application of the porous polyethylene films derived from cocontinuous blends as supports for gas separation membranes, compatibilized blends with PE-*g*-MA are better candidates: they have smaller more stable pores and more wettable interfaces.

Extrusion Experiments. The objective of twin-screw corotating extrusion experiments was to see if the process could be scaled up from the microcompounder. The effect of blend composition, residence time and shear rate on the morphology of cocontinuous blends was investigated. Residence time was manipulated by introducing the PEO in either zone 1 or zone 5, which corresponded to 80 and 50 s for lower shear configuration and 120 and 70 s for high shear configuration, respectively. Note that PE-*g*-MA was always introduced in zone 1. Shear rate was altered by implementing

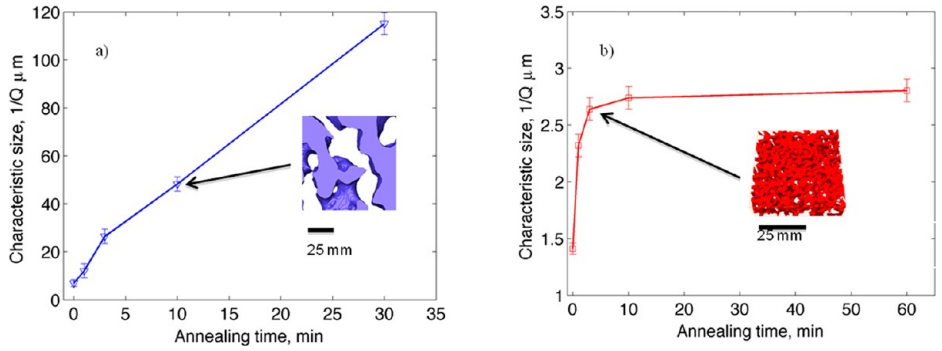

Figure 5. Inverse of interfacial area per unit volume ($1/Q$) vs annealing time of 50/50 vol % blends: (a) PEO/PE blend, (b) PEO/PE-*g*-MA blend.

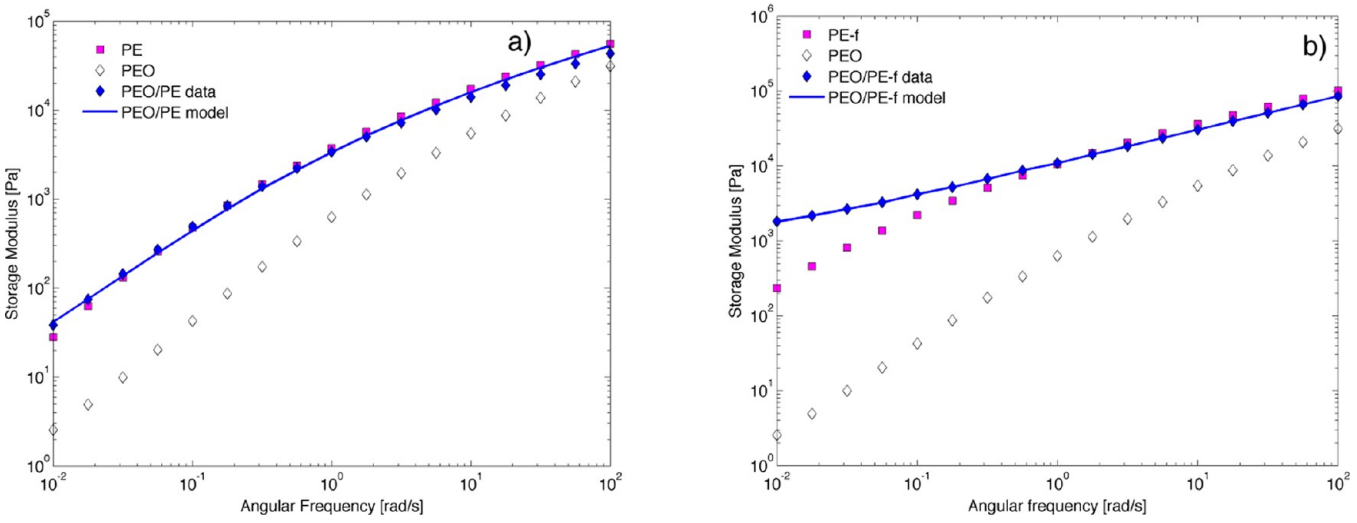

Figure 6. Storage modulus vs frequency of the pure polymers and 90/10 PE/PEO wt % blends. From Palierne model fit for (a) PE/PEO blend, R_{avg}= 1.02 μm, Γ = 3 mN/m and for (b) PE-*g*-MA/PEO blend, R_{avg} = 0.15 μm, Γ = 0.4 mN/m.

two different screw configurations. The main difference was a block of high-shear kneading elements after zone 5 in the high shear screw, as opposed to a block of conveying elements in the low-shear configuration[23] (see Supporting Information).

Figure 7 summarizes the effect of the aforementioned factors on the characteristic length, as calculated from 3D images and eq 1. As seen from Figure 7, 50/50 blend compositions give the smallest characteristic length, $1/Q$.

On average, the low shear configuration resulted in a smaller $1/Q$. For both low and high shear screws error bars associated with zone 5 (shorter residence times) were larger. The difference in the uniformity of the blends obtained by introducing PEO in zone 1 vs zone 5 was obvious even by the naked eye.

In order to quantify the uniformity of these blends, the pore size distribution was calculated using the stack of binarized 2D images acquired by LSCM via the calculation procedure described in the Experimental Section. Figure 8 depicts the equivalent diameter pore size distribution of 50/50 vol % PE-*g*-MA/PEO blends obtained by the two different screws and residence times.

It is evident that shorter residence times (PEO introduced in zone 5) result in broader pore size distribution for both high- and low-shear screw configuration. Also, high-shear results in larger pores for both residence times, which can be attributed to shear induced pore coalescence. Note that the characteristic length, $1/Q$, calculated from 3D images was comparable to the

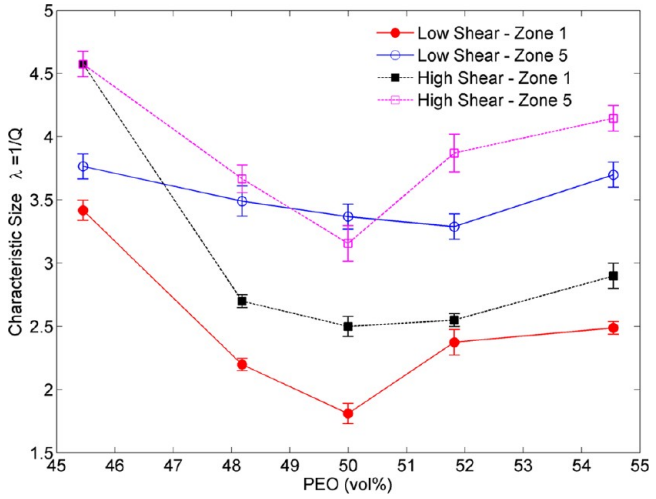

Figure 7. Characteristic length as a function of blend composition, shear rate, and PEO zone introduction. Residence time for low shear screw, zone 1 addition = 80 s; low shear, zone 5 = 40 s; high shear screw, zone 1 addition = 120 s; high shear, zone 5 = 70 s.

average equivalent pore diameter, D_{eq}, obtained from LSCM images. As previously mentioned, D_{eq} represents the diameter of a circle with the same area as the pore. Quantitative differences between D_{eq} and $1/Q$ can be explained by the fact

dx.doi.org/10.1021/ma300293v | *Macromolecules* 2012, 45, 6036−6044

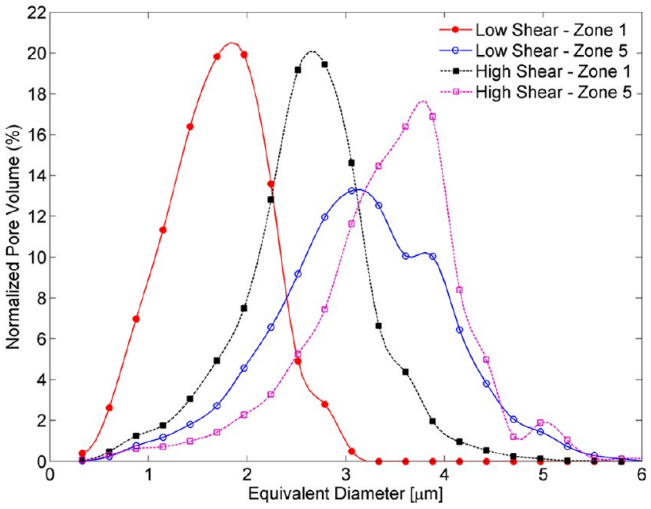

Figure 8. Equivalent diameter pore size distribution 50/50 vol % PE-*g*-MA/PEO blend as a function of shear rate and PEO zone introduction. Residence time for low shear screw, zone 1 addition = 80 s; low shear, zone 5 = 40 s; high shear, zone 1 = 120 s; high shear, zone 5 = 70 s.

that the shapes of pores vary from circular to very elongated and irregular.

Burst Pressure Experiments. In order to study the mechanical robustness of the developed porous polymer films, the burst pressure of the gas separation membranes was tested in a diffusion cell. The membrane was placed between the two compartments of a diffusion cell, described previously.[36] The top chamber can be pressurized up to 10 atm, and the bottom chamber is at atmospheric pressure at the beginning of the experiment.

Gas separation membranes were prepared by filling the pores of PE sheets with an ion gel composed of poly(vinylidene fluoride-*co*-hexafluoropropylene) (p(VDF−HFP)) swelled with (1-ethyl-3-methylimidazolium bis(trifluoromethylsulfonyl)-imide ([EMIM][TFSI]), 20/80 w/w. This ionic gel has promising properties in gas separation of CO_2/CH_4 and CO_2/N_2 gas pairs, with the real selectivity being nearly the same as the ideal selectivity.[21] The procedure consisted of solvent casting an acetone solution of the ion gel into porous PE sheets followed by acetone evaporation under vacuum. The main purpose of the support layer is to provide mechanical strength and prevent the ionic gel being extruded out under the pressure difference. Therefore, small average pore size and uniform pore size distribution are desirable. Once the membrane was prepared, it was clamped in the diffusion cell, and both compartments were thoroughly flushed with CO_2 gas. The top chamber was pressurized, and the bottom chamber was at the atmospheric pressure at the beginning of the experiment. The pressure in the top chamber was increased in increments of 0.5 atm, and pressures in both chambers were continuously monitored in 1 s intervals. Burst pressure was defined as the pressure under which pressures in both chambers suddenly equilibrated.

Typical examples of porous polyethylene sheets employed as support for gas separation membranes are depicted in Figure 9. Figure 9a represents the SEM micrograph of porous PE film derived from the extruder blend with low shear configuration and longer residence time (PEO introduced in zone 1), Figure 9b shows the micrograph of porous PE film from the extruder blend with low-shear configuration and shorter residence time (PEO introduced in zone 5), and Figure 9c presents the porous PE sheet generated from uncompatibilized blends (PEO introduced in zone 1). Their corresponding measured burst pressures in the diffusion cell are >10, 4.5, and <1 atm, respectively. The results were in agreement with our previous characterization of extruder blends in terms of characteristic length (Figure 7) and pore size distribution (Figure 8) and also the morphology differences shown in Figure 9. Blends obtained with longer residence time in the extruder result in smaller average pore size, but also more uniform pore size distribution. Consequently, the membranes designed using these films as supports could withstand the maximum allowable gas pressure by the experimental setup. However, blends with shorter residence time result in wider pore size distribution (Figures 8 and 9b) and a significantly lower maximum gas pressure. Lastly, uncompatiblized blends result in large pore size, and no significant pressure difference could be applied without extruding the ionic gel out of the porous film. Thus, the burst pressure is a function of average pore size as well as the coefficient of variation in pore size distribution. Understanding the precise functionality of the burst pressure and the failure mechanism of the gas separation membranes will be the object of future experimental studies coupled with finite elements modeling.

CONCLUSION

PE/PEO cocontinuous polymer blends were successfully prepared using a batch microcompounder and a twin-screw extruder and employed as a support layer for gas separation membranes. Blends prepared from PE-*g*-MA showed dramat-

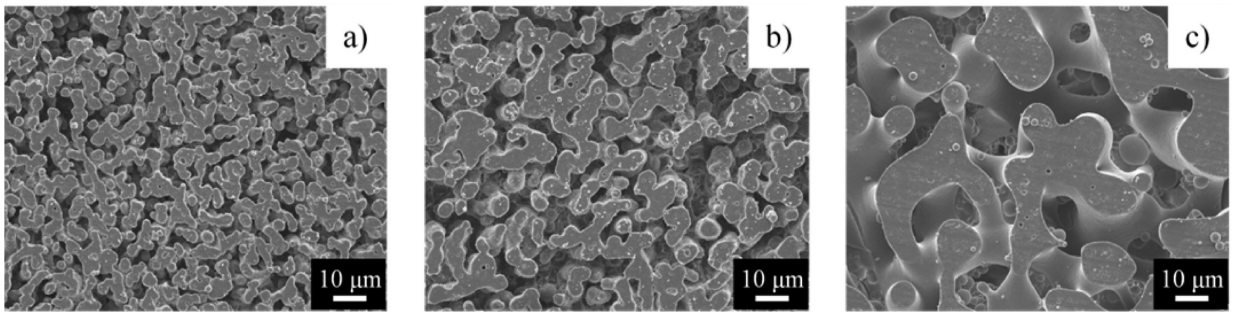

Figure 9. SEM micrographs of 50/50 vol % cocontinuous blends: (a) PE-*g*-MA/PEO, 80 s residence time (burst pressure >10 atm); (b) PE-*g*-MA/PEO, residence time 40 s (burst pressure = 4.5 atm); (c) PE/PEO residence time 80 s (burst pressure <1 atm). All samples compounded with low-shear screw configuration.

ically smaller phase sizes when compared to blends prepared from nonfunctional PE. Smaller phase size was attributed to reactive coupling of the OH groups on PEO with the anhydride groups on PE-*g*-MA resulting in reduced interfacial tension. The Palierne viscoelastic droplet model was used for determining the interfacial tension, which was estimated to be 3 mN/m in nonreactive PE/PEO system and 0.4 mN/m in reactive PE-g-MA/PEO system. The specific interfacial area was calculated from the triangular mesh data of interface between the two phases, and a MATLAB code was developed for calculation of the pore size distribution based on the 3D image data. Aside from the importance of minimizing the average pore size, pore size distribution was found to play a role in the performance of the derived porous polymer films as supports in gas separation membranes. Decreasing the residence time in the twin-screw extruder by changing the PEO zone introduction (for both shear configurations) resulted in the broader pore size distribution. Consequently, these films were less mechanically robust and could not withstand maximum allowable gas pressure in the diffusion cell. On the other hand, longer residence time allowed more effective blending of two polymers and yielded smaller average pore size and narrower pore size distribution.

■ ASSOCIATED CONTENT

Supporting Information

Figures 10 and 11. This material is available free of charge via the Internet at http://pubs.acs.org.

■ AUTHOR INFORMATION

Corresponding Author

*E-mail: macosko@umn.edu.

Notes

The authors declare no competing financial interest.

■ ACKNOWLEDGMENTS

This work was supported by the MRSEC Program of the National Science Foundation, NSERC (Natural Sciences and Engineering Research Council of Canada), and CONII (Colleges Ontario Network for Industry Innovation). Parts of this work were carried out in the Characterization Facility, University of Minnesota, which receives partial support from NSF through the MRSEC program. Image acquisition was carried out in the Biomedical Image Processing Laboratory and the image processing and analysis at the Minnesota Supercomputing Institute at the University of Minnesota.

■ REFERENCES

(1) Scott, C. E.; Macosko, C. W. Morphology Development During the Initial Stages of Polymer-Polymer Blending. *Polymer* **1995**, *36*, 461−470.

(2) Tucker, C. L., III; Moldenaers, P. Microstructural evolution in polymer blends. *Annu. Rev. Fluid Mech.* **2002**, *34*, 177−210.

(3) Pötschke, P.; Paul, D. R. Formation of co-continuous structures in melt-mixed immiscible polymer blends. *J. Macromol. Sci., Part C: Polym. Rev.* **2003**, *43* (1), 87−141.

(4) Guo, H.; Packirisamy, S.; Mani, R.; Aronson, C.; Gvozdic, N.; Meier, D. Compatibilizing effects of block copolymers in low-density polyethylene/polystyrene blends. *Polymer* **1998**, *39* (12), 2495−2505.

(5) Asthana, H.; Jayaraman, K. Rheology of reactively compatibilized polymer blends with varying extent of interfacial reaction. *Macromolecules* **1999**, *32* (10), 3412−3419.

(6) Baker, W.; Scott, C.; Hu, G. H. *Reactive Polymer Blending*; Hanser Publishers: Munich, Germany, 2001.

(7) Galloway, J.; Jeon, H. K.; Bell, J. R.; Macosko, C. W. Block copolymer compatibilization of cocontinuous polymer blends. *Polymer* **2005**, *46* (1), 183−191.

(8) Yuan, Z.; Favis, B. D. Coarsening of immiscible co-continuous blends during quiescent annealing. *AIChE J.* **2005**, *51* (1), 271−280.

(9) Lopez-Barron, C. R.; Macosko, C. W. Coarsening of PS/SAN blends with cocontinuous morphology studied with 3D image analysis. *Macromol. Symp.* **2009**, *283*−*284* (1), 348−353.

(10) Bell, J. R.; Chang, K.; López-Barrón, C. R.; Macosko, C. W.; Morse, D. C. Annealing of cocontinuous polymer blends: effect of block copolymer molecular weight and architecture. *Macromolecules* **2010**, *43* (11), 5024−5032.

(11) Doi, M.; Ohta, T. Dynamics and rheology of complex interfaces. *J. Chem. Phys.* **1991**, *95* (2), 1242−1248.

(12) Lopez-Barron, C. R.; Macosko, C. W. Characterizing interface shape evolution in immiscible polymer blends via 3D image analysis. *Langmuir* **2009**, *25* (16), 9392−404.

(13) Jinnai, H.; Nishikawa, Y.; Spontak, R. J.; Smith, S. D.; Agard, D.; Hashimoto, T. Direct measurement of interfacial curvature distributions in a bicontinuous block copolymer morphology. *Phys. Rev. Lett.* **2000**, *84* (3), 518−21.

(14) Sengupta, P.; Noordermeer, J. W. M. Three-dimensional structure of olefinic thermoplastic elastomer blends using electron tomography. *Macromol. Rapid Commun.* **2005**, *26* (7), 542−547.

(15) Momose, A.; Fujii, A.; Kadowaki, H.; Jinnai, H. Three-dimensional observation of polymer blend by X-ray phase tomography. *Macromolecules* **2005**, *38* (16), 7197−7200.

(16) Pyun, A.; Bell, J. R.; Won, K. H.; Weon, B. M.; Seol, S. K.; Je, J. H.; Macosko, C. W. Synchrotron X-ray microtomography for 3D imaging of polymer blends. *Macromolecules* **2007**, *40*, 2029−2035.

(17) Koizumi, S.; Yamane, Y.; Kuroki, S.; Ando, I.; Nishikawa, Y. Three-dimensional observation of phase-separated poly (methyl methacrylate)/ poly (styrene-ran-4- bromostylene) blends by 3D NMR microscopy with X-ray microscopy. *Polymer* **2006**, *103*, 470−475.

(18) Verhoogt, H.; Dam, J. V.; de Boer, A. P.; Draaijer, A.; Houpt, P. M. Confocal laser scanning microscopy: a new method for determination of the morphology of polymer blends. *Polymer* **1993**, *34*, 1325−1329.

(19) Palierne, J. E. Linear rheology of viscoelastic emulsions with interfacial tension. *Rheol. Acta* **1990**, *214*, 204−214.

(20) Gu, Y.; Lodge, T. P. Synthesis and gas separation performance of triblock copolymer ion gels with a polymerized ionic liquid midblock. *Macromolecules* **2011**, *44*, 1732−1736.

(21) Jansen, J. C.; Friess, K.; Clarizia, G.; Schauer, J.; Izak, P. High ionic liquid content polymeric gel membranes: preparation and performance. *Macromolecules* **2010**, *44*, 39−45.

(22) Macosko, C. M. *Rheology Principles, Measurements, and Applications*; Wiley-VCH: New York, 1994.

(23) Trifkovic, M.; Sheikhzadeh, M.; Choo, K.; Rohani, S. Model predictive control of a twin-screw extruder for thermoplastic vulcanizate (TPV) applications. *Comput. Chem. Eng.* **2012**, *36*, 247−254.

(24) Ridler, T.; Calvard, S. Picture thresholding using an iterative selection method. *IEEE Trans. Syst., Man, Cybernetics* **1978**, *8*, 630−632.

(25) López-Barrón, C. R.; Macosko, C. W. Direct measurement of interface anisotropy of bicontinuous structures via 3D image analysis. *Langmuir* **2010**, *26* (17), 14284−14293.

(26) Mather, M. L.; Morgan, S. P.; White, L. J.; Tai, H.; Kockenberger, W.; Howdle, S. M.; Shakesheff, K. M.; Crowe, J. A. Image-based characterization of foamed polymeric tissue scaffolds. *Biomed. Mater.* **2008**, *3* (1), 1−11.

(27) Wenzel, R. N. Resistance of solid surfaces to wetting by water. *Ind. Eng. Chem.* **1936**, *28*, 988−994.

(28) Lacroix, C.; Bousmina, M.; Carreau, P. J.; Favis, B. D.; Michel, A. Properties of PETG/EVA blends: 1. Viscoelastic, morphological and interfacial properties. *Polymer* **1996**, *37* (14), 2939−2947.

(29) Gramespacher, H. Interfacial tension between polymer melts measured by shear oscillations of their blends. *J. Rheol.* **1992**, *36* (6), 1127−1136.
(30) Mekhilef, N.; Carreau, P. J.; Favis, B. D.; Martin, P.; Ouhlal, A. Viscoelastic properties and interfacial tension of polystyrene-polyethylene blends. *J. Polym. Sci., Part B: Polym. Phys.* **2000**, *38* (10), 1359−1368.
(31) Xing, P.; Bousmina, M.; Rodrigue, D.; Kamal, M. R. Critical experimental comparison between five techniques for the determination of interfacial tension in polymer blends: model system of polystyrene/polyamide-6. *Macromolecules* **2000**, *33* (21), 8020−8034.
(32) Jacobs, U.; Fahrländer, M.; Winterhalter, J.; Friedrich, C. Analysis of Palierne's emulsion model in the case of viscoelastic interfacial properties. *J. Rheol.* **1999**, *48*, 1495−1509.
(33) Van Hemelrijck, E.; Van Puyvelde, P.; Velankar, S.; Macosko, C. W.; Moldenaers, P. Interfacial elasticity and coalescence suppression in compatibilized polymer blends. *J. Rheol.* **2004**, *48*, 143−158.
(34) Tselios, Ch.; Bikiaris, D.; Prinos, J.; Panayiotou, C. Structure and properties of blends of poly(ethylene-co-vinyl alcohol) with poly(styrene-co-maleic anhydride). *J. Appl. Polym. Sci.* **1997**, *64* (5), 983−999.
(35) Flores, M.; Hernandez, G.; Escobar, A.; Cardoso, J.; Palma, A.; Maciel, A.; Sanchez, E.; Manero, O. Synthesis and processing of the (ethylene-vinyl acetate-vinyl alcohol) terpolymer and its blends with a polyamide and styrene copolymers. *J. Appl. Polym. Sci.* **1998**, *67* (7), 1071−1083.
(36) Phillip, W. A.; Rzayev, J.; Hillmyer, M. A.; Cussler, E. L. Gas and water liquid transport through nanoporous block copolymer membranes. *J. Membr. Sci.* **2006**, *286*, 144−152.